



Observation of the Sagittarius dwarf galaxy with H.E.S.S.

J. MASBOU¹, A. CHARBONNIER², A. JACHOLKOWSKA², G. LAMANNA¹, S. ROSIER-LEES¹, JP. TAVERNET², P. VINCENT².

¹*Laboratoire d'Annecy-le-Vieux de Physique des Particules, Universit de Savoie/CNRS/IN2P3 F-74941 Annecy-le-Vieux, France*

²*LPNHE, Universite Pierre et Marie Curie Paris 6, Universite Denis Diderot Paris 7, CNRS/IN2P3, 4 Place Jussieu, F-75252, Paris Cedex 5, France*

masbou@lapp.in2p3.fr

DOI: 10.7529/ICRC2011/V05/1078

Abstract: Dwarf spheroidal galaxies are among the most promising candidates for the indirect searches of Dark Matter particle annihilation signals due to a large measured Mass-to-Light ratio and expected absence of potential astrophysical background. The annihilation of dark matter particles in the center of Sagittarius dwarf spheroidal (Sgr dSph) galaxy would produce high energy gamma-rays in the final state. The High Energy Stereoscopic System (H.E.S.S.) of Imaging Atmospheric Cherenkov Telescopes (IACTs) located in Namibia is in operation since December 2003. With more than 40 hours of data acquired by H.E.S.S. on the Sagittarius dwarf spheroidal galaxy and in absence of a clear signal, new constraints on the annihilation cross-section of the Dark Matter particles are derived in the framework of SUSY models.

Keywords: IACT, Dwarf Spheroidal galaxy, Dark Matter

1 Introduction

The existence of dark matter is currently assumed in the Standard Cosmological Model with approximately 22% [1] of the overall mass-energy budget of the universe. It is also supported by a large amount of observations such as rotation curves in the spiral galaxies and velocity dispersion in the elliptical galaxies, gravitational lensing and large scale distribution of galaxies. However, the nature of the particle that constitute the dark matter remains unknown. Among many theoretical candidates for the DM particle, a Weakly Interacting Massive Particle (WIMP) is among the best motivated. Such candidates for WIMPs are predicted in theories beyond the Standard Model of particle physics [2]. Here we consider the lightest neutralino provided by supersymmetric extensions of the Standard Model, with R-parity conservation [3].

A pairs of dark matter particles can annihilate and produce Standard Model particles. Direct annihilations into $\gamma\gamma$ or $Z\gamma$ produce a sharp line spectrum with a photon energy depending on the neutralino mass. Unfortunately, these processes are loop-suppressed and therefore very rare. Dark matter can also annihilate to pairs of leptons or quarks, leading in subsequent processes to π^0 decays, resulting in a continuous photon spectrum.

Assuming the Λ CDM cosmological model, the hierarchical collapse of small overdensities are formed by dark matter structures. Dark matter structures may also host

smaller satellite structures and it has been proposed that dwarf spheroidal galaxies may have formed within some of these subhalos hosted in the larger Milky Way dark matter halo [5]. The core of the Sagittarius Dwarf Spheroidal Galaxy (Sgr dSph) is located at $l=5.6^\circ$ and $b=-14.1^\circ$ in galactic coordinates at a distance of about 24 kpc from the Sun [4].

The High Energy Stereoscopic System (H.E.S.S.) is an array of four Imaging Atmospheric Cherenkov Telescopes (IACTs) for high energy gamma-rays, designed for high sensitivity measurements in the 100 GeV - 10 TeV energy range. It is a suitable instrument to detect very high energy gamma-rays and potentially originated by WIMPs annihilation.

In this paper, we present the observations of Sgr dSph by the H.E.S.S. array then the signal extraction procedure. The results on gamma detection and constraints on the velocity-weighted annihilation cross-section in the frame of supersymmetric models is presented.

2 H.E.S.S. observations

The H.E.S.S. array, in the southern hemisphere, is composed of four IACTs which allow the use of the stereoscopic technique. Associated to the great collection surface (107 m^2) of each telescope and fine pixellisation of cameras (960 PMTs per camera), the system leads to an excel-

lent rejection of hadronic background produced by charged cosmic rays. It provides a sensitivity to a 1% of the Crab Nebula flux in ~ 25 h observation [6].

Gamma-rays and hadronic showers are reconstructed from their images in Cherenkov lights using three different methods. The first one is based on the Hillas parameters [6] characterizing each image globally. The second one is based on the comparison between the registered shower images and a predicted pixel-by-pixel modeling of the expected image within a realistic detector simulation [7]. The third method is based on a three-dimensional elliptical reconstruction of the gamma-ray induced air shower on the basis of their rotational symmetry with respect to the incident direction [8]. The procedure in use relies on a composed estimator X_{eff} [9] of the discriminating variables provided by the three different methods. This combination relies on the maximum information obtained from each reconstruction in use in H.E.S.S. and gives competitive results on signal-to-background discrimination, important for searches of tiny exotic signals. The energy resolution obtained is $\sim 10\%$ and the angular resolution lower than 0.08° .

H.E.S.S. has observed Sgr dSph in the 2006-2010 period. The observation were performed in wobble mode, i.e. with the target offset by 0.7° . to 1.1° . from the pointing direction, allowing simultaneous background estimation in the same field-of-view. The data used for the analysis were taken at average zenith angles of 20° . The data are analyzed with the X_{eff} analysis tuned to look for faint source ('*detection*') with an angular size for the candidate source of $\theta^2 \leq 0.02^\circ$. The effective energy threshold is 460 GeV, defined as the energy for which the acceptance of the instrument reaches 20% of its maximum value. The observation time is 44.7 hours after quality selection criteria.

3 The dark matter annihilation signal

The gamma-ray flux due to dark matter particle annihilations depends on:

1. the intrinsic dark matter density distribution in the source,
2. the particle physics coupling of the dark matter particle,
3. the field of view $\Delta\Omega$ within which the signal is integrated.

It is usually factorized in two terms:

$$\frac{d\Phi_\gamma}{dE_\gamma}(E_\gamma, \Delta\Omega) = \Phi^{PP}(E_\gamma) \times J(\Delta\Omega) \Delta\Omega \quad (1)$$

The first factor take into account the particle physics of dark matter particle annihilations. The second factor, called J-factor, is about the astrophysics with the distribution of dark matter in the source.

3.1 The particle physics factor

The particle physics factor Φ^{PP} is given by:

$$\Phi^{PP}(E_\gamma) \equiv \frac{d\Phi_\gamma}{dE_\gamma} = \frac{1}{8\pi} \frac{\langle \sigma_{ann} v \rangle}{m_\chi^2} \times \frac{dN_\gamma}{dE_\gamma}, \quad (2)$$

where $\langle \sigma_{ann} v \rangle$ is the velocity averaged annihilation cross section, m_χ is the DM particle mass, and dN_γ/dE_γ is the differential gamma-ray spectrum summed over the whole final states with their corresponding branching ratios. In this paper, all the results are based on an average spectrum, the Bergstrom parametrisation [10]:

$$\frac{dN_\gamma}{dE_\gamma} = \frac{1}{m_\chi} \frac{dN_\gamma}{dx} = \frac{1}{m_\chi} \frac{0.73 e^{-7.8x}}{x^{1.5}} \quad (3)$$

with $x \equiv E_\gamma/m_\chi$.

3.2 The astrophysical part: J-factor

In the astrophysical factor, the integral along the line-of-sight (l.o.s.) of the squared density of the dark matter distribution in the object is averaged over the instrument solid angle of the integration region. For this analysis with H.E.S.S., $\Delta\Omega = 2 \times 10^5$ sr since we are looking for an almost pointlike signal considering the point-spread function of the instrument:

$$J = \frac{1}{\Delta\Omega} \int_{\Delta\Omega} \int \rho_{DM}^2(l, \Omega) dl d\Omega. \quad (4)$$

Two different modeling of the dark matter halo [11] of Sgr dSph have been previously considered without considering its disruption by tidal winds. With recent measurements, Niederste-Ostholt et al. [12] estimate that only 30 - 50% of the luminosity of Sgr dSph remains currently bound in the remnant core. New modeling of Sgr dSph now exist taking into account tides.

An isothermal profile for dark matter halo is considered by Peñarrubia et al. [13] assuming that Sgr dSph is a late-type, rotating disc galaxy. In this model, the galaxy is composed of a stellar disk and a dark matter component with the following density distribution:

$$\rho_{ISO}(r) = \frac{m_h \alpha}{2\pi^{3/2} r_{cut}} \frac{\exp[-(r/r_{cut})^2]}{(r_c^2 + r^2)}, \quad (5)$$

where m_h is the halo mass, r_c is the core radius and $\alpha \simeq 1.156$. It is found that the properties of the stream are not particularly sensitive to the value of the core radius choose at $r_c = 0.45$ kpc. Assuming a initial luminosity of $\sim 10^8 L_\odot$ [12] and a mass-to-light ratio of 24 [14], the total mass of the halo is found to be $m_h = 2.4 \times 10^9 M_\odot$. To take into account the lost of the outer halo envelope due to tidal disruption by the Milky Way, a truncation in the dark matter density profile is imposed at $r_{cut} = 12 r_c = 5.4$ kpc. It roughly corresponds to the tidal radius of a satellite galaxy a pericenter of 15 kpc with a mass $\sim 3 \times 10^9 M_\odot$.

Dark matter profile	J-factor [GeV ² .cm ⁻⁵]
Isothermal	0.88×10^{23}
NFW	1×10^{23}

Table 1: J-factor computed for the two different dark matter halo profiles.

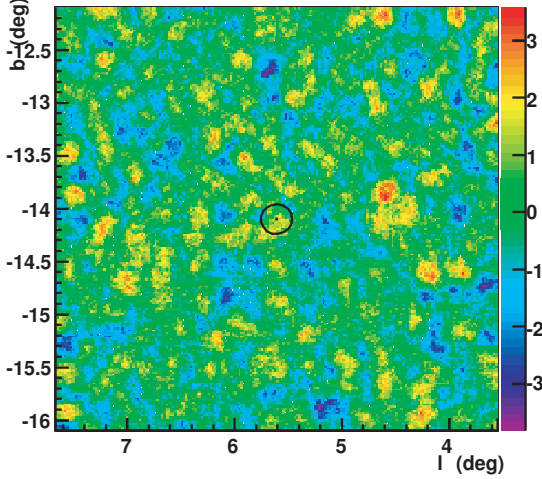


Figure 1: Significance sky map of the SgrD region. No excess is observed at the target position: $l=5.6^\circ$ and $b=-14.1^\circ$ in galactic coordinates. The integration region is in the black circle. Other spots in the field of view are not significant.

Cosmological simulations support an other type of dark matter halo which can be described by a NFW profile [15]:

$$\rho_{\text{NFW}}(r) = \frac{\rho_s}{(r/r_s)(1+r/r_s)^2} \quad (6)$$

where parameter values [16]: $r_s = 1.3$ kpc is a scale radius and $\rho_s = 1.1 \times 10^{-2} M_\odot \text{pc}^{-3}$ is a characteristic density.

The J-factor can be computed using the equation 4. They are summarised in table 1.

4 Results

No significant gamma ray excess was found above the estimated backgrounds at the nominal positions of Sgr dSphs, as presented in figure 1. The target position is chosen according to the photometric measurements of the Sgr dSph luminous cusp showing that the position of the center corresponds to the center of the globular cluster M 54 [17]: (RA = 18h55m59.9s, Dec = -30d28'59.9") in equatorial coordinates (J2000.0). A 95% confidence level upper limits on the total observed numbers of gamma-rays is computed $N_{\gamma}^{\text{95\%C.L.}}$. The limits is computed using the number of events in the signal and background regions normalized by the ratio between the on-source area and the off-

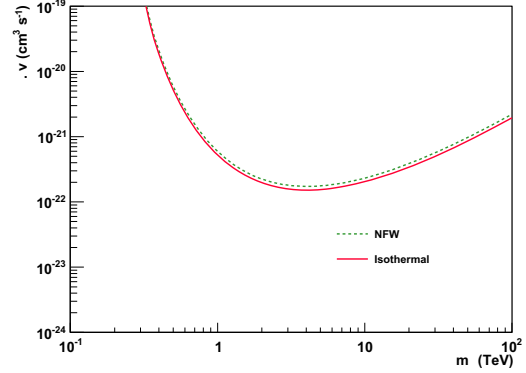


Figure 2: Upper limit at 95% C.L. on $\langle \sigma_{\text{ann}} v \rangle$ versus the dark matter particle mass in the case of a cusp NFW (green dotted line) and a cored isothermal dark matter halo profile (red line).

source area. The Feldman & Cousins [18] methods gives $N_{\gamma}^{\text{95\%C.L.}} = 41 \gamma$.

The 95% C.L. upper limit on the velocity-weighted annihilation cross section as function of the DM particle mass for a given halo profile is given by:

$$\langle \sigma v \rangle_{\text{min}}^{\text{95\% C.L.}} = \frac{8\pi}{J(\Delta\Omega)\Delta\Omega} \times \frac{m_{\text{DM}}^2 N_{\gamma, \text{tot}}^{\text{95\% C.L.}}}{T_{\text{obs}} \int_0^{m_{\text{DM}}} A_{\text{eff}}(E_\gamma) \frac{dN_\gamma}{dE_\gamma}(E_\gamma) dE_\gamma} \quad (7)$$

where T_{obs} is the observation time of the source, $A_{\text{eff}}(E_\gamma)$ is the H.E.S.S. effective area and the parametrization of dN_γ/dE_γ is the Bergstrom parametrisation. The exclusion curve for the neutralino is plotted for Sgr dSph in Figure 2 referring to the halo profiles given in the table 1. The exclusion limits are $\sim 10^{-22} \text{ cm}^3 \cdot \text{s}^{-1}$, above the benchmark value of $\langle \sigma_{\text{ann}} v \rangle \sim 3 \times 10^{-26} \text{ cm}^3 \cdot \text{s}^{-1}$ [3]. As the two J-factor are similar, the limits are at the same order.

5 Summary

The H.E.S.S. observations reveal no significant excess of gamma-rays at the nominal position of Sgr dSph. The latest modeling of Sgr dSph halo have been used to estimated its structure parameter and compute the J-factor. Constraints have been derived on the velocity-weighted cross section of the dark particle in the framework of supersymmetric model.

References

- [1] E. Komatsu et al., *Astrophys. J. Suppl.*, 2011, **192**(18)
- [2] G. Bertone, D. Hooper, J. Silk, *Phys. Rept.*, 2005, **405**: 279-390

- [3] G. Jungman, M. Kamionkowski, K. Griest, *Phys. Rept.*, 1996, **267**: 195-373
- [4] S. R. Majewski, *Astrophys. J.*, 2003, **599**: 1082-1115
- [5] A. V. Kravtsov, O. Y. Gnedin, A. A. Klypin, *Astrophys. J.*, 2004, **609**: 482-497
- [6] F. Aharonian et al. (H.E.S.S. Collaboration), *A&A*, 2006, **457**: 899-915
- [7] M. de Naurois, L. Rolland, *Astropart. Phys.*, 2009, **32**(5): 231-252
- [8] M. Lemoine-Goumard, B. Degrange, M. Tluczykont, *Astropart. Phys.*, 2006, **25**(3): 195-211
- [9] F. Dubois, G. Lamanna, A. Jacholkowska, *Astropart. Phys.*, 2009, **32**(2): 73-88
- [10] L. Bergstrom, P. Ullio, J. H. Buckley, *Astropart. Phys.*, 1998, **9**(2): 137-162
- [11] F. Aharonian et al. (H.E.S.S. Collaboration), *Astropart. Phys.*, 2008, **29**: 55-62, Erratum 2010, **33**: 274-275
- [12] M. Niederste-Ostholt, V. Belokurov, N. W. Evans, J. Peñarrubia, *Astrophys. J.*, 2010, **712**(1): 516-526
- [13] Peñarrubia et al., *MNRAS*, 2010, **408**(1): L26-L30
- [14] M. L. Mateo, *ARA&A*, 1998, **36**: 435-506
- [15] J. F. Navarro, C. S. Frenk, D. M. White, *Astrophys. J.*, 1996, **462**: 563
- [16] A. Viana et al., arXiv:1103.2627v1 [astro-ph.HE]
- [17] L. Monaco et al., *MNRAS*, 1995, **356**(4): 1396-1402
- [18] G. J. Feldman, R. D. Cousins, *Phys. Rev. D*, 1998, **57**(7): 3873-3889